

RESEARCH ON CORNEAL STRUCTURE

A strong interplay between theory and experiment is a key feature in our continuing development of light scattering as a probe of corneal structure. A general theory for predicting scattering from the structures depicted in electron micrographs of abnormal corneas is reviewed, and an experimental test verifying that collagen fibrils are the primary scattering elements in the cornea is presented.

INTRODUCTION

The Milton S. Eisenhower Research Center has a long-standing interest in understanding the properties of the cornea. Earlier investigations were reviewed in two previous *Technical Digest* articles.^{1,2} The initial work¹ demonstrated that the order in the spatial arrangements of the fibrillar ultrastructure depicted in electron micrographs could produce the interference effects needed to explain transparency, and that macromolecular models in which fibrils are linked by mucoprotein bridges were consistent with the electron micrographs. In a subsequent study,² a strong interplay between theory and experiment was used to develop light scattering as a probe of the ultrastructure in fresh corneal tissue and to explain infrared damage to corneal cells. In what follows, we review briefly a general theory that we developed to predict light scattering using electron micrographs of abnormal corneas³ and an experimental verification that fibrils are the primary scattering elements.⁴ The theory applies to arbitrary inhomogeneous distributions of parallel fibrils having an arbitrary distribution of fibril diameters. The experimental test is based on the prediction that the differential scattering cross section, normalized appropriately, should follow a universal curve that depends on wavelength λ and scattering angle θ_s , only through the combination $\lambda/\sin(\theta_s/2)$.

BACKGROUND

The cornea is the transparent part of the eye's outer sheath (Fig. 1) and the primary refractive element in the optical system of the eye. Indeed, its curved interface with the air provides three-fourths of the eye's focusing power (the remainder being provided by the lens). Maintenance of its curvature and clarity is therefore essential for good vision. The structural elements that give the cornea the strength to preserve its proper curvature while withstanding the intraocular pressure (typically 14 to 18 mm Hg) are located within its stromal region, which constitutes 90% of the cornea's thickness.⁵ The stroma comprises many layers of stacked sheets called lamellae, which average $\approx 2 \mu\text{m}$ in thickness. A few flat cells (keratocytes) are dispersed between the lamellae, and these occupy 3% to 5% of the stromal volume. Each lamella is composed of a parallel array of collagen fibrils surrounded by an optically homogeneous solution consisting of water, mucoproteins, and various salts⁵ (see

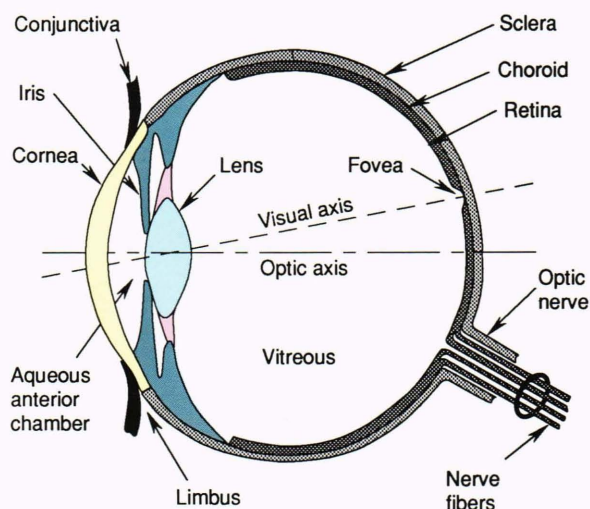


Figure 1. A diagram of the eye showing the location of the curved, transparent cornea.

Figs. 2 and 3). The fibrils have nearly uniform diameters, averaging $\approx 30 \text{ nm}$ in man, and extend entirely across the cornea (lying essentially parallel to its surface), where they enlarge and blend into the white sclera at the limbus. The fibril axes in adjacent lamellae tend to make large angles with one another. This fibrillar structure gives the cornea its required strength.

The refractive index of the fibrils differs from that of their surroundings; most estimates of the relative index m range from 1.05 to 1.10.^{1,2,5-7} Because of this difference and because the fibrils are so numerous, it was recognized long ago that if they acted as independent scattering elements, they would scatter so much light that the cornea would be opaque.⁸ Thus, modern theories predict that the cornea's transparency results from an ordered spatial arrangement of the fibrils that creates essentially complete destructive interference among the waves scattered in all but the forward direction.^{1,5-14}

The visibility of the cornea in the ophthalmologist's slit lamp demonstrates that it is not perfectly transparent. In fact, the cornea actually scatters about 2% of the red light and about 10% of the blue light incident on it.¹⁵ The characteristics of this small amount of scattered light contain information about the structural ele-

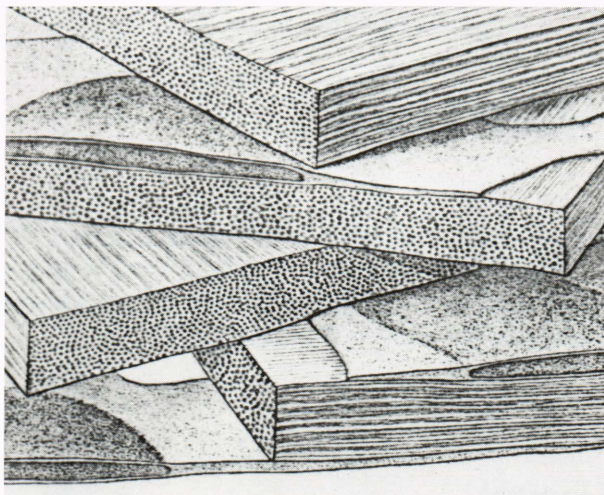


Figure 2. A schematic illustration of several lamellae from a normal cornea. The collagen fibrils are of uniform diameter and, within a given lamella, are all parallel to each other and run the entire breadth of the cornea. The lamellae are oriented at various angles with respect to each other. Three keratocytes are also shown between the lamellae. (Reprinted, with permission, from Hogan, M. J., Alvarado, J. A., and Weddell, J. E., *Histology of the Human Eye*, p. 93, Philadelphia, 1971; © 1971 by W. B. Saunders.)

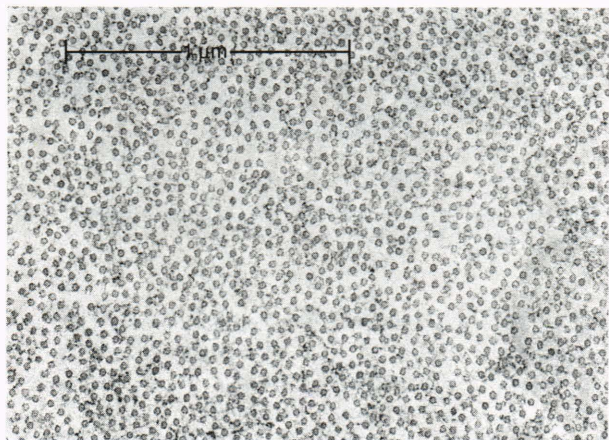


Figure 3. Electron micrograph showing the fibrils within the stroma of a normal rabbit cornea.

ments from which the light is scattered, thereby permitting us to combine theory and experiment to develop light scattering as a tool for probing the stroma's ultrastructure.^{2,4,12-16} The general approach, which has been quite successful, is to characterize corneas through measurement and analysis of their light scattering properties. By comparing experimental scattering data and theoretical predictions based on structures depicted in electron micrographs, model structures, or both, we can test the validity of the structures.

Previously we devised methods to calculate the scattering expected from the distributions of collagen fibrils depicted in electron micrographs of the normal cornea, such as that shown in Figure 3.^{1,6,7} We showed that the fibril positions could be described by a radial distribu-

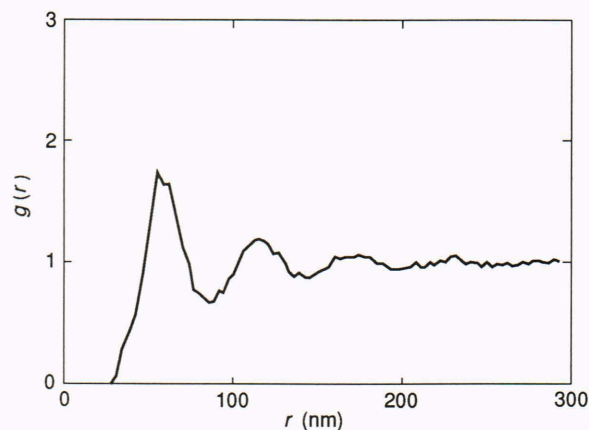


Figure 4. The radial distribution function, $g(r)$, for the fibrils shown in Figure 6. This function is the ratio of the local number density of fibrils at a distance r from an arbitrary fibril to the overall bulk number density; it represents the probability of finding a fibril a distance r from any given fibril and goes to unity at large distances.

tion function, $g(r)$, an example of which is presented in Figure 4. Thus, the theory developed for X-ray scattering in liquids^{17,18} could be applied. In swollen or damaged corneas, however, we cannot describe fibril distributions in this way, and consequently the earlier theory is not valid. The following section describes our efforts to devise a calculation procedure based on a direct summation of fields from the measured positions of fibril centers in electron micrographs.³ This procedure would be applicable to swollen or damaged corneas as well as normal corneas, and would also enable one to account explicitly in the calculations for the wide variability of fibril diameters that has been reported in certain types of scars.¹⁹

The various models developed to explain corneal transparency, as well as our development of light scattering as a probe of fibrillar structure, rest on the fundamental assumption that the collagen fibrils are the primary source of scattering in the stroma. On the basis of this assumption, models to explain corneal transparency and its loss when the cornea swells have been analyzed and tests devised to discern among them, especially on the basis of the predicted wavelength dependencies of scattering.^{2,12,15} Although experiments continue to support the theories that are based on the structures revealed by electron microscopy, we must remember that stromal structure is complex, and other potential sources of scattering, such as cells, are present. Such an important hypothesis, therefore, should be subjected to whatever tests can be devised. In a subsequent section of this article, we examine the experimental conditions for which the hypothesis is valid (and those for which it is not, *viz.*, specular scattering), and describe an experimental test of a theoretical prediction of how angular scattering scales with light wavelength and scattering angle.⁴ Experiments confirm the predicted scaling relationship, which provides additional strong support for the idea that the collagen fibrils are the principal scatterers, except at specular scattering angles.⁴

DIRECT SUMMATION-OF-FIELDS METHOD

The underlying problem is to calculate the field that would be scattered by L stacked sheets composed of fibrils embedded in a ground substance. In general, the total scattered field \mathbf{E}_s can be written as

$$\mathbf{E}_s = \sum_{l=1}^L \mathbf{E}_s(l) , \quad (1)$$

where $\mathbf{E}_s(l)$ is the field scattered by the fibrils in the l th lamella. The scattered intensity equals the absolute square of the scattered field, so that

$$I = \sum_{l=1}^L |\mathbf{E}_s(l)|^2 + \sum_{l=1}^L \sum_{\substack{m=1 \\ m \neq l}}^L \mathbf{E}_s(l) \cdot \mathbf{E}_s^*(m) , \quad (2)$$

where $*$ denotes complex conjugation.

As with the Zernike-Prins-type analysis developed in Ref. 6, we evaluate the average intensity for an ensemble of corneas of a given type. We assume that the l th lamella of the corneas in the ensemble all have the same bulk number density of fibril axes and the fibril positions and diameters are distributed similarly, but that the specific position of fibrils, in general, differs throughout the ensemble. The field scattered from the l th lamella can depend on that from the m th lamella in two ways, namely, if the positions of their fibrils are correlated or if multiple scattering is important. For the cornea, fibril positions in different lamellae are uncorrelated, and we are primarily interested in semitransparent tissues for which multiple scattering can be neglected. Thus, the Born approximation in which the field experienced by the fibrils is replaced by the incident field can be used, and one finds

$$\langle I \rangle = \sum_{l=1}^L \langle |\delta \mathbf{E}_s(l)|^2 \rangle + \left| \langle \sum_{l=1}^L \mathbf{E}_s(l) \rangle \right|^2 , \quad (3a)$$

where $\langle \rangle$ denotes the ensemble average, and

$$\delta \mathbf{E}_s(l) \equiv \mathbf{E}_s(l) - \langle \mathbf{E}_s(l) \rangle . \quad (3b)$$

Although the members of the ensemble have similar spatial distributions of fibrils, the actual positions in different members of the ensemble are uncorrelated. Thus, $\langle \sum_{l=1}^L \mathbf{E}_s(l) \rangle$ is the field that would be scattered by a perfectly homogeneous cornea. Its absolute square represents the diffraction that would arise from the finite-sized illuminated region. This diffraction term depends only on the overall size and shape of the illuminated region and is negligible (except in the forward direction) for typical profiles of the incident beam intensity.

We obtain the scattering from fibrils by neglecting the second term in Equation 3a, so that

$$\langle I \rangle = \sum_{l=1}^L Q(l) , \quad (4a)$$

with

$$Q(l) \equiv \langle |\delta \mathbf{E}_l|^2 \rangle . \quad (4b)$$

In principle, we could evaluate $Q(l)$ by averaging over many corneas; however, we devised a method for approximating it from an electron micrograph of a single lamella. We first place a grid consisting of $M(l)$ rectangular boxes over the l th lamella (cf. Fig. 5) and write $\delta \mathbf{E}_l$ as

$$\delta \mathbf{E}_l = \sum_{j=1}^{M(l)} \delta \mathbf{E}_l^{(j)} , \quad (5)$$

where, analogous with Equation 3b, $\delta \mathbf{E}_l^{(j)}$ is the field scattered by the fibrils in the j th box minus the ensemble average field that would be scattered by fibrils within such a box. If the boxes are made large compared with the correlation length, then correlations among fibrils in different boxes can be neglected, and Equation 4b can be written as

$$Q(l) = \sum_{j=1}^{M(l)} \langle |\delta \mathbf{E}_l^{(j)}|^2 \rangle \quad (6a)$$

$$= M(l) \left[\langle |\mathbf{E}_l^{(r)}|^2 \rangle - |\langle \mathbf{E}_l^{(r)} \rangle|^2 \right] , \quad (6b)$$

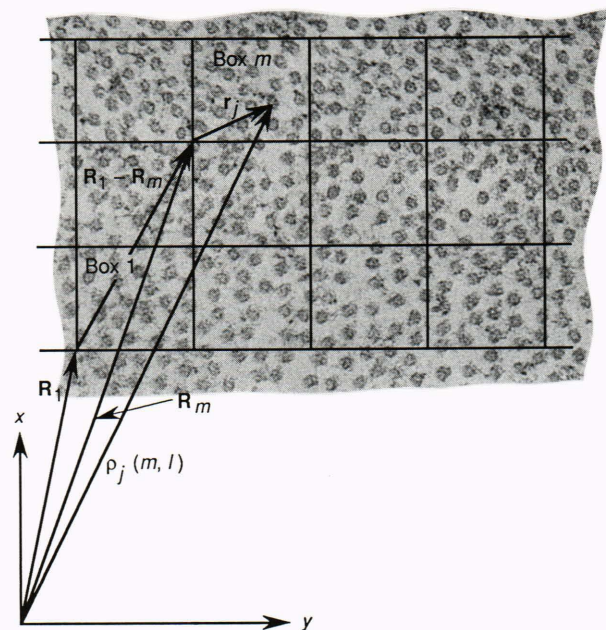


Figure 5. Hypothetical grid placed over a lamella. The fixed, arbitrary coordinate system is used to locate fibril centers ρ_j and boxes \mathbf{R}_m . An illustrative translation is shown for box 1 and box m ; box 1 corresponds to the reference box.

where we have used the facts that the ensemble average of $|\delta\mathbf{E}_l^{(j)}|^2$ is independent of the particular box, j , and $\langle |\delta\mathbf{E}_l^{(j)}|^2 \rangle = \langle |\mathbf{E}_l^{(j)}|^2 \rangle - |\langle \mathbf{E}_l^{(j)} \rangle|^2$. The superscript r in Equation 6b denotes a generic or reference rectangular box.

We can approximate the ensemble average in Equation 6 from the fibril distributions in the K boxes of that portion of the grid covering the fibrils depicted in an electron micrograph. Specifically, we choose one box as the reference rectangle and treat the other $(K - 1)$ boxes as if they were the reference box from other corneas in the ensemble. This identification requires that the other boxes be translated so that they overlap the reference box. In the Born approximation, the field scattered by a fibril located at a position \mathbf{r}_j is of the form

$$\mathbf{E}_{sc} = \mathbf{E}_{sc}^{(0)} \exp(i\mathbf{q} \cdot \mathbf{r}_j) , \quad (7)$$

where $\mathbf{E}_{sc}^{(0)}$ is the field that would be scattered from the fibril if its axis were at the origin, $\mathbf{q} = \mathbf{k}_i - \mathbf{k}_s$ (\mathbf{k}_i and \mathbf{k}_s being the wave vectors of the incident and scattered waves), and we have assumed that the detector is not in the near field of the scatterer. From the form of Equation 7, one can show that the effect of the above translation is to introduce a phase factor $\exp\{i\mathbf{q} \cdot [\mathbf{R}_r - \mathbf{R}_m]\}$ in the scattered field, where \mathbf{R}_r and \mathbf{R}_m locate a reference point (e.g., the lower left-hand corner) in the reference and m th box, respectively (cf. Fig. 5). Thus, an unbiased estimate for $Q(l)$ can be obtained from

$$Q(l) = \frac{M(l)K}{(K - 1)} \left[\overline{\mathbf{E}_r^2} - \overline{\mathbf{E}_r}^2 \right] , \quad (8a)$$

where the bars denote sample average, specifically,

$$\overline{\mathbf{E}_r^2} = \frac{1}{K} \sum_{m=1}^K |e^{i\mathbf{q} \cdot (\mathbf{R}_r - \mathbf{R}_m)} \mathbf{E}_m|^2 , \quad (8b)$$

and

$$\overline{\mathbf{E}_r} = \frac{1}{K} \sum_{m=1}^K e^{i\mathbf{q} \cdot (\mathbf{R}_r - \mathbf{R}_m)} \mathbf{E}_m . \quad (8c)$$

The phase factor $e^{i\mathbf{q} \cdot (\mathbf{R}_r - \mathbf{R}_m)}$ is included in Equation 8b to emphasize the translation, and the factor $K/(K - 1)$ in Equation 8a arises because the sample average field $\overline{\mathbf{E}_r}$ differs from the ensemble average field $\langle \mathbf{E}_r \rangle$.

The field scattered by the fibrils within the m th box, \mathbf{E}_m , is the sum of the fields scattered by the individual fibrils within it. The latter fields depend on fibril positions through the phase factor in Equation 7, and their dependence on the fibril diameter and refractive index is contained in $\mathbf{E}_{sc}^{(0)}$ (of that equation), which can be calculated from the series solution. For the normal and swollen corneas discussed here, all fibrils have essentially the same diameter and refractive index, and the field \mathbf{E}_m is given by

$$\mathbf{E}_m = \mathbf{E}_{sc}^{(0)} \sum_{j=1}^{N(m)} e^{i\mathbf{q} \cdot \mathbf{r}_j} \equiv \mathbf{E}_{sc}^{(0)} S_m(\lambda, \theta_s) , \quad (9)$$

where the summation is over the $N(m)$ fibrils in the m th box, and $S_m(\lambda, \theta_s)$ is the phase sum, which depends on scattering angle θ_s and light wavelength λ .

The application of Equation 4a to calculate transmission through normal and swollen corneas can be simplified by noting that, for total scattering, the layered nature of the cornea can be ignored since, for unpolarized light, the *total* scattering from each fibril is independent of its azimuthal orientation. As we will emphasize in the following section, the azimuthal orientations profoundly affect angular scattering and must be considered in analyzing measurements of angular scattering. For transmission, however, the cornea can be treated as a single lamella whose thickness is that of the entire cornea. The total cross section is obtained by integrating the differential (or angular) cross section over scattering angles. With these assumptions, the differential scattering cross section per fibril becomes

$$\sigma_s(\lambda, \theta_s) = \frac{\sigma_0(\lambda, \theta_s)K}{(K - 1)\overline{N}_r} \left\{ \overline{|S_r(\lambda, \theta_s)|^2} - \overline{|S_r(\lambda, \theta_s)|}^2 \right\} , \quad (10)$$

where

$\sigma_0(\theta_s) \equiv |\mathbf{E}_{sc}^{(0)}|^2/|E_0|^2$ is the differential scattering cross section for an isolated fibril, $|E_0|^2$ is the intensity of the incident beam, the barred quantities within the brackets are sample average values of the phase sums defined in analogy to Equations 8b and 8c, and \overline{N}_r is the sample average number of fibrils within the reference box.

The calculation is performed by first recording the coordinates of the fibril centers from a micrograph of a region in a single lamella. The sample average of the phase sums in Equation 10 is evaluated over a series of angles θ_s between 0 and 2π for various wavelengths, and then $\sigma_s(\lambda, \theta_s)$ is integrated numerically between 0 and 2π to obtain the total scattering cross section per fibril per unit length, σ_{tot} . The fraction of light transmitted through the cornea is then found from the relation

$$F_T = \exp(-\rho\Delta\sigma_{tot}) , \quad (11)$$

where ρ is the number density of fibril centers in the lamella, and Δ is the thickness of the cornea.^{2,6-7} In Ref. 3, we performed this calculation for the large region indicated in Figure 6 and compared the results with those obtained using the earlier formulation based on the radial distribution function.^{6,7} The results, plotted in Figure 7, show excellent agreement between the two



Figure 6. Electron micrograph of a region in the central stroma of a normal rabbit cornea that was fixed while applying a transcorneal pressure of 18 mm Hg. The large rectangle indicates the area of the lamella used for analysis.

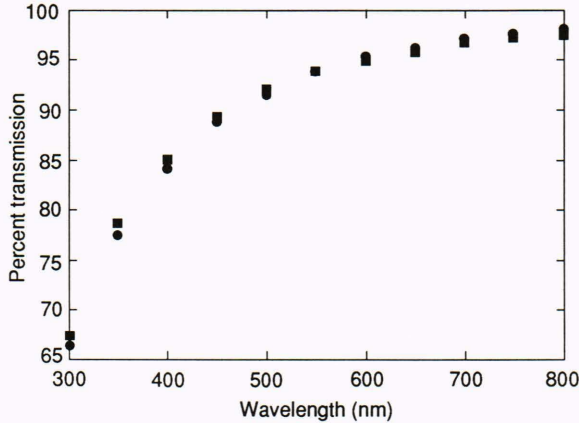


Figure 7. Calculated light transmission plotted as a function of wavelength. The circles were computed by the direct summation of fields for a grid with 157 fibrils per box. The squares were computed using the radial distribution function.

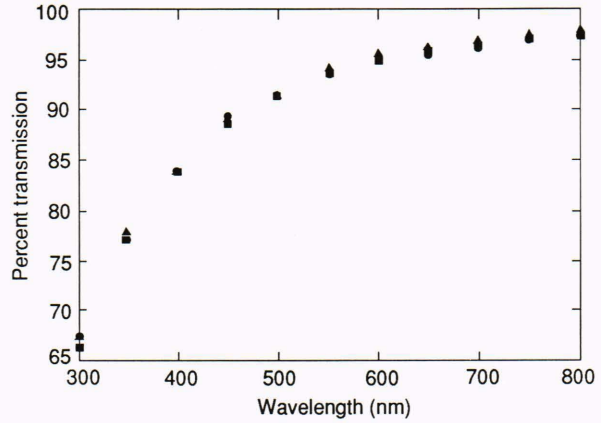


Figure 8. Calculated light transmission plotted as a function of wavelength. The squares were computed from the entire region using a grid with 157 fibrils per box. The circles were computed from the entire region using a grid with 1262 fibrils per box. The triangles were computed from a subregion using a grid with 10 boxes containing 162 fibrils per box. The results are virtually identical for all three computations.

methods. (Previously we showed that the calculations based on the radial distribution function agreed closely with experimental determinations of the fraction transmitted.^{6,7,15}) Figure 8 shows that the calculations are independent of grid size, thus supporting our assumption that correlations between boxes could be ignored if the box size was larger than the correlation length. In addition, Figure 8 shows that accurate results can be obtained from a subregion that is closer in size to typical micrographs (cf. Fig. 3).

We have also used the method to calculate scattering from a micrograph (Fig. 9) of a cornea that was swollen to 1.25 times its initial thickness.²⁰ Again, the fibril positions in swollen corneas cannot be described by a radial distribution function, and, therefore, scattering from such micrographs could not be calculated before now. The predicted transmission closely agrees with measured values (taken from Ref. 15); but, more importantly, Figure 10 shows that the wavelength dependence of the total scattering cross section agrees with the measured value. The figure shows that σ_{tot} contains a term that varies as λ^{-2} , which agrees with our extension of Benedek's lake theory.^{2,9,12-15} This agreement between the calculated and measured values suggests that the small voids (or lakes) noted in the micrograph (Fig. 9) are not artifacts of the preparation method.

STROMAL SCATTERING

Specular Versus Nonspecular Scattering

In addition to the matrix of collagen fibrils, other possible sources of scattering in the stroma are cells and un-



Figure 9. Electron micrograph of the stroma from the posterior region of a 25% swollen rabbit cornea.

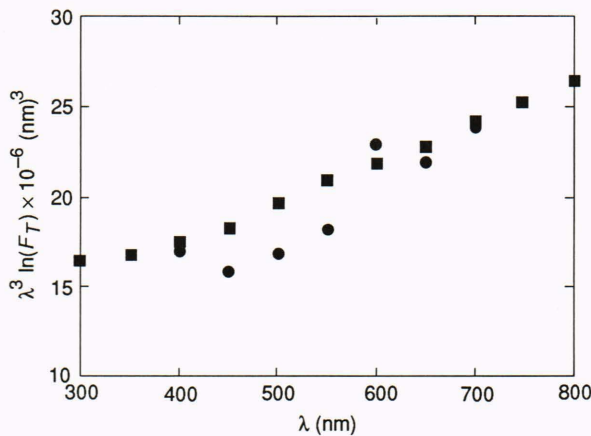


Figure 10. Comparison of calculated (■) and measured (●) values of $\lambda^3 \ln|F_T|$ as a function of wavelength for a 25% swollen rabbit cornea. Multiplication by the cube of the wavelength removes the inverse cubic dependence that characterizes the individual fibril cross section. The straight line of positive slope indicates the increased effect of scattering by lakes in swollen corneas, which, according to our extension of Benedek's theory,¹⁵ contributes a term proportional to λ^{-2} .

undulations in the lamellae that exist at low intraocular pressures when the tension in the fibrils is relaxed. These undulations are the source of the small angle scattering patterns that we discussed in a previous *Technical Digest* article and elsewhere.^{2,16,21} To understand the relative importance of these possible sources of scattering, it is instructive to view the cornea in the scattering apparatus (shown in Fig. 11) under different conditions of illumination. In Figure 12A the incident light is normal to the central cornea, and the scattering angle θ_s is 120° . The bands at the front and back surfaces are caused by scattering from the epithelial and endothelial

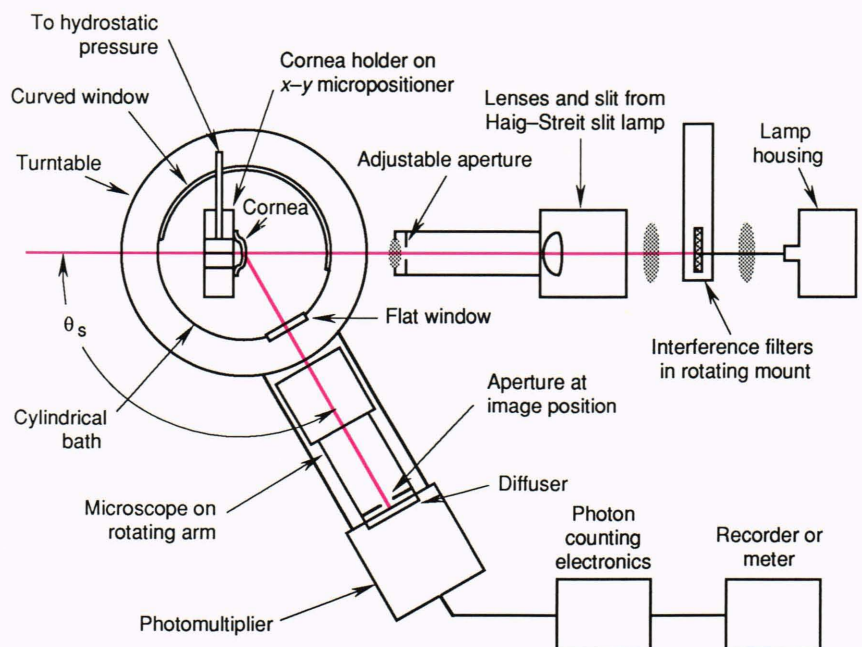
cell layers, respectively. The stromal region contains a few bright "flecks," which presumably are scattering from cells, on a diffuse background, which presumably represents the scattering from the fibrillar matrix. This appearance is typical at all scattering angles for this setup. Figure 12B shows the same cornea shifted laterally to produce specular scattering at $\theta_s = 144^\circ$. (Here, the incident light is no longer normal to the corneal surface.) In this photograph, which received 13 times less exposure than the one in Figure 12A, the cells in the stroma shine intensely against a darker background. Scattering from the cellular layers at the front and back of the cornea also is much more intense in Figure 12B.

We obtain a similar result when we view the stroma with a scanning-slit specular microscope. This instrument, lent to us by David Maurice of Stanford University, operates using the same principles now employed in confocal microscopes and, as configured here, isolates a thin optical section of the stroma ($\approx 2 \mu\text{m}$ thick).²² Figure 12C shows a representative view in the stroma in which the bright ovals are keratocytes, and the complex background pattern arises from the lamellar undulations found at low intraocular pressures. Similar patterns have been observed and reported by Gallagher and Maurice.²³ We see from Figures 12B and 12C that the flat keratocytes, which have lateral dimensions of several wavelengths, act like tiny mirrors under the condition of specular reflection and dominate the scattering. The specular condition must therefore be avoided in scattering experiments designed to probe fibrillar structures.

Tests for Fibrillar Scattering—Nonspecular Scattering

The idea for a test to determine whether stromal scattering derives primarily from fibrils comes directly from

Figure 11. Schematic diagram of the experimental scattering apparatus.



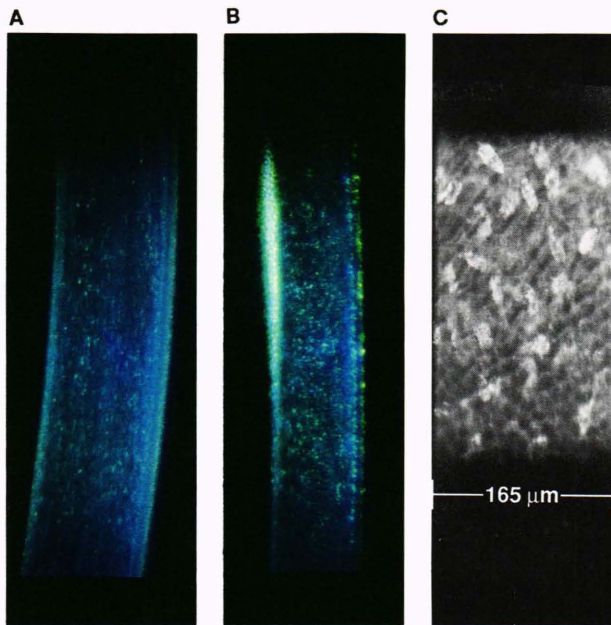


Figure 12. Three different views of a cornea. **A.** Scattering at $\theta_s = 120^\circ$ from a rabbit cornea, with the incident light normal to the surface as viewed in the scattering apparatus shown in Figure 11. **B.** Scattering at $\theta_s = 144^\circ$ from the same rabbit cornea, except that it has been shifted laterally; the incident light is no longer normal to the cornea's surface. Scattering from stromal cells and the front and back cellular layers of the cornea is much more intense. This photograph received 13 times less exposure than the one in Figure 12A. **C.** The cornea viewed with a scanning-slit specular microscope. The bright ovals are keratocytes, and the background pattern is caused by lamellar undulations.

our earlier theory based on the radial distribution function. As discussed in the previous section, this theory treated the stroma as a single lamella of parallel, infinitely long fibrils, which for this discussion we take to be aligned perpendicular to the scattering plane defined by the incident beam and the axis of the collection optics (cf. Fig. 11). We defined the azimuthal angle of this plane measured from the vertical to be $\phi_s = \pi/2$. We then showed that, if the fibril diameters were small compared with the wavelength, the scattering intensity (per unit length) could be expressed as⁶

$$I_s(\theta_s, \pi/2) = \frac{AI_0}{r_s} \left(\frac{1 + B \cos^2 \theta_s}{\lambda^3} \right) \left\{ 1 - 2\pi\rho \times \int_0^{R_c} r dr [1 - g(r)] J_0[2kr \sin(\theta_s/2)] \right\}, \quad (12)$$

where

- I_0 is the intensity of the incident light,
- r_s is the distance to the field point,
- A is a constant having dimensions (length),⁴ which depends on the diameter and dielectric properties of the fibrils,
- B is a dimensionless constant, which depends on the relative refractive index of the fibrils and their surroundings,

R_c is the distance over which fibril positions are correlated,

ρ is the number density of fibrils in the lamella, k is the magnitude of the incident wave vector, and J_0 is the 0th-order Bessel function of the first kind.

From Equation 12 we clearly see that if the scattering were primarily from a single lamella of parallel fibrils, the quantity

$$S(\lambda, \theta_s) \equiv \frac{\lambda^3 [I_s(\theta_s, \pi/2) / I_0]}{1 + B \cos^2 \theta_s} \quad (13)$$

should scale with wavelength and scattering angle via an effective wave number

$$k_{\text{eff}} \equiv k \sin(\theta_s/2). \quad (14)$$

In a real cornea, however, the nature of scattering from long cylinders requires that the azimuthal orientations of the fibrils in the different layers of the stroma be considered in deriving an expression for angular scattering. Scattering from an infinitely long cylinder is a cylindrically outgoing wave, with the wave vector of the scattered wave orthogonal to the cylinder axis at all points along its (infinite) length. For finite cylinders, the situation is similar at intermediate distances, where the scattering is also a cylindrically outgoing wave confined to the narrow band, which is defined by the height of the illuminated region of the cylinder (assumed here to be much smaller than the size of the detector). In the far field, the scattering peaks sharply about the plane that is perpendicular to the cylinder axis and passes through its center. When using the apparatus shown in Figure 11 to measure angular scattering, therefore, only those lamellae whose fibrils are oriented to within a certain tilt angle from the scattering plane (defined by the incident beam and the optic axis of collection optics) will contribute to the measured scattering. We see this schematically in Figure 13, which also shows that the number of these lamellae varies with the scattering angle θ_s . In Ref. 4, we used these considerations to derive the proper form of Equation 12, which accounts for the azimuthal orientations of the stromal lamellae, the net result being that the form of the constant A is slightly different, and an additional factor of $\sin \theta_s$ appears in the denominator. Thus, the quantity that should scale with k_{eff} is $\sin \theta_s S(\lambda, \theta_s)$ and not simply $S(\lambda, \theta_s)$.

We used the scattering apparatus in Figure 11 to test this relationship. For the measurements, the corneas were bathed in normal saline solution (0.154 molar concentration of NaCl) and maintained at an intraocular pressure of 18 mm Hg. Measurements were made at scattering angles of 35° , 40° , 50° , 60° , 115° , 120° , 130° , 140° , and 150° and at the four strong lines in the mercury arc's visible spectrum, 404.7, 435.8, 546.1, and 577.7 nm. Full experimental details can be found in Ref. 4. The results are plotted in Figure 14, where we used a value of 1.09

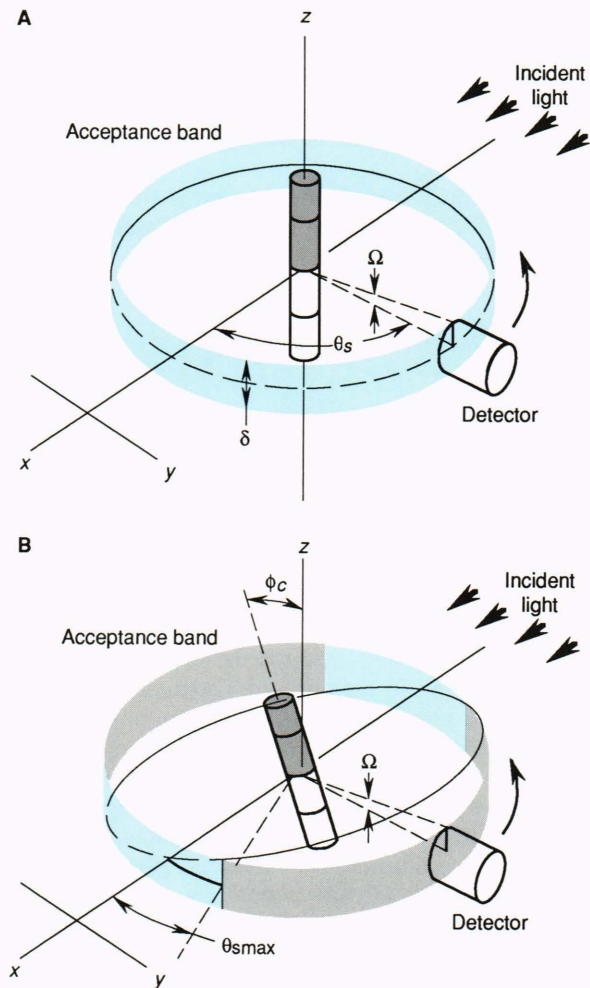


Figure 13. A schematic representation of scattering from a cylindrical fibril. **A.** This geometry shows the finite acceptance band δ resulting from the angular acceptance of the detection optics. The scattering from the fibril, which is oriented perpendicular to the x - y plane, is confined to directions very near that plane, whose intersection with the acceptance band is indicated by the solid and dashed line (the angular spread of the scattering out of the plane is much less than the detector acceptance angle Ω). Scattering from such a fibril would be detected at all scattering angles θ_s . **B.** Scattering from a fibril lying in the y - z plane, but tilted at an angle ϕ_c with respect to the z axis, is essentially confined to the plane through its center, which makes an angle ϕ_c with the x - y plane. The intersection of this plane with the top of the acceptance band defines the maximum scattering angle in the forward direction θ_{smax} for which a fibril tilted at an angle ϕ_c would contribute to the measured signal. Similarly, the intersection also defines the minimum scattering angle in the backward direction $\pi - \theta_{smax}$ for which such a fibril would contribute (scattering angles θ_s are measured between 0 and π). For scattering angles $\theta_{smax} \leq \theta_s \leq \pi - \theta_{smax}$, the scattering misses the acceptance band. From these considerations, it is obvious that all fibrils (or lamellae) would contribute to the measured scattering at $\theta_s = 0$ or π , whereas at $\theta_s = \pi/2$, the number of contributing lamellae diminishes to those having tilt angles $< \Omega$.

for the relative refractive index m to determine the constant $B = 4/(m^2 + 1)$ in Equation 13. All of the values collapse to a single curve, indicating that the predicted scaling is observed.

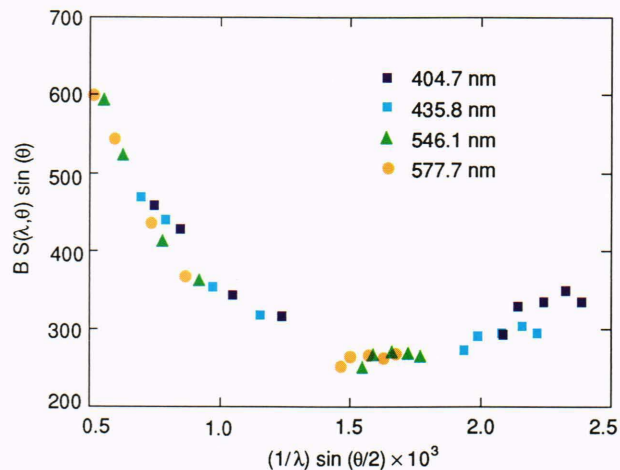


Figure 14. Experimental measurements of the function $\sin \theta_s S(\lambda, \theta_s)$, defined in Equation 13, plotted as a function of k_{eff} . These data are the average values from four normal rabbit corneas. The observed scaling agrees with the hypothesis that fibrils are the primary source of nonspecular light scattering in the cornea.

This confirmation of the scaling provides additional, strong evidence that the matrix of collagen fibrils is the primary source of scattering in the corneal stroma. Thus, transparency theories, which are all based on this assumption, remain on firm ground. Further, our continued use of light scattering to probe fibrillar structures in the stroma is justified.

REFERENCES

- Hart, R. W., Farrell, R. A., and Langham, M. E., "Theory of Corneal Structure," *APL Tech. Dig.* **8**, 2-11 (1969).
- Farrell, R. A., Barger, C. B., Green, W. R., and McCally, R. L., "Collaborative Biomedical Research on Corneal Structure," *Johns Hopkins APL Tech. Dig.* **4**, 65-79 (1983).
- Freund, D. E., McCally, R. L., and Farrell, R. A., "Direct Summation of Fields for Light Scattering by Fibrils with Applications to Normal Corneas," *Appl. Opt.* **25**, 2739-2746 (1986).
- Freund, D. E., McCally, R. L., and Farrell, R. A., "Effects of Fibril Orientations on Light Scattering in the Cornea," *J. Opt. Soc. Am. A* **3**, 1970-1982 (1986).
- Maurice, D. M., "The Cornea and Sclera," in *The Eye*, Vol. 1B, Davson, H., ed., Academic Press, Orlando (1984).
- Hart, R. W., and Farrell, R. A., "Light Scattering in the Cornea," *J. Opt. Soc. Am.* **59**, 766-774 (1969).
- Cox, J. L., Farrell, R. A., Hart, R. W., and Langham, M. E., "The Transparency of the Mammalian Cornea," *J. Physiol. (Lond.)* **210**, 601-616 (1970).
- Maurice, D. M., "The Structure and Transparency of the Corneal Stroma," *J. Physiol. (Lond.)* **136**, 263-286 (1957).
- Benedek, G. B., "The Theory of Transparency of the Eye," *Appl. Opt.* **10**, 459-473 (1971).
- Feuk, T., "On the Transparency of the Stroma in the Mammalian Cornea," *IEEE Trans. Biomed. Eng.* **BME-17**, 186-190 (1970).
- Twersky, V., "Transparency of Pair-Related, Random Distributions of Small Scatterers, with Applications to the Cornea," *J. Opt. Soc. Am.* **65**, 524-530 (1975).
- Farrell, R. A., and McCally, R. L., "On Corneal Transparency and Its Loss with Swelling," *J. Opt. Soc. Am.* **66**, 342-345 (1976).
- McCally, R. L., and Farrell, R. A., "Interaction of Light and the Cornea: Light Scattering versus Transparency," in *The Cornea: Transactions of the World Congress on the Cornea III*, Cavanagh, H. D., ed., Raven Press, New York (1988).
- McCally, R. L., and Farrell, R. A., "Light Scattering from Cornea and Corneal Transparency," in *New Developments in Noninvasive Studies to Evaluate Ocular Function*, Masters, B., ed., Springer-Verlag, New York (in press, 1990).

- ¹⁵Farrell, R. A., McCally, R. L., and Tatham, P. E. R., "Wavelength Dependencies of Light Scattering in Normal and Cold Swollen Rabbit Corneas and Their Structural Implications," *J. Physiol. (Lond.)* **233**, 589-612 (1973).
- ¹⁶McCally, R. L., and Farrell, R. A., "Structural Implications of Small-Angle Light Scattering from Cornea," *Exp. Eye Res.* **34**, 99-111 (1982).
- ¹⁷Zernike, F., and Prins, J. A., "Die Beugung von Röntgenstrahlen in Flüssigkeiten als Effekt der Molekulanordnung," *Z. Phys.* **41**, 184 (1927).
- ¹⁸Debye, P., and Menke, H., "Bestimmung der Inneren Struktur von Flüssigkeiten mit Röntgenstrahlen," *Phys. Z* **31**, 797 (1930).
- ¹⁹Schwarz, W., and Graf Keyserlingk, D., "Electron Microscopy of Normal and Opaque Human Cornea," in *The Cornea*, Langham, M. E., ed., The Johns Hopkins Press, Baltimore (1969).
- ²⁰McCally, R. L., Freund, D. E., and Farrell, R. A., "Calculations of Light Scattering from EM of Swollen Corneas by Direct Summation of Fields," *Invest. Ophthalmol. Vis. Sci. (Supplement)* **27**, 350 (1986).
- ²¹Andreo, R. H., and Farrell, R. A., "Corneal Small-Angle Light Scattering Patterns: Wavy Fibril Models," *J. Opt. Soc. Am.* **72**, 1479-1492 (1982).
- ²²Maurice, D. M., "A Scanning Slit Optical Microscope," *Invest. Ophthalmol.* **13**, 1033-1037 (1974).
- ²³Gallagher, B., and Maurice, D. M., "Striations of Light Scattering in the Corneal Stroma," *J. Ultrastruct. Res.* **61**, 100-114 (1977).

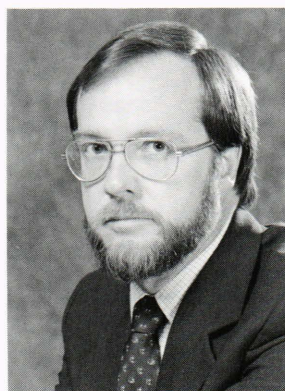
ACKNOWLEDGMENTS: This work was supported in part by the National Eye Institute (Grant EY01019), by the U.S. Army Medical Research and Development Command, and by the U.S. Navy under Contract N00039-89-C-5301. We thank James Cox (Wilmer Institute of the Johns Hopkins Medical Institutions), who did the electron microscopy; Ray Wisecarver (McClure Computing Center), who digitized the fibril locations in Figure 6; and Ujjal Ghoshtagore, who, as a summer apprentice, digitized and helped analyze the results from the micrograph in Figure 9. Special thanks are due to Stanley Favin (Mathematics and Information Science, APL), who aided in the development of the computer programs for the direct summations method, and to Robert W. Hart, who gave valuable insights on the effects of fibril orientations.

THE AUTHORS



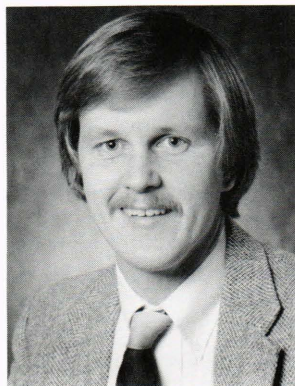
RICHARD A. FARRELL is a principal staff physicist and supervisor of the Theoretical Problems Group in APL's Milton S. Eisenhower Research Center. Born in Providence, Rhode Island, he obtained a B.S. degree from Providence College in 1960, an M.S. degree from the University of Massachusetts in 1962, and a Ph.D. degree from The Catholic University of America in 1965. Dr. Farrell's research interests include relating the cornea's structure to its function, developing theoretical methods for calculating wave scattering in random media, analyzing the statistical mechanics of phase

transitions, and modeling ocular blood flow. He has been involved in collaborative efforts with the Johns Hopkins Medical School since joining APL in 1965. Dr. Farrell is the principal investigator on a grant from the National Eye Institute and recently served on their steering committee for a workshop on corneal biophysics. He is a member of the American Physical Society, the Optical Society of America, the Association for Research in Vision and Ophthalmology, the International Society for Eye Research, and the New York Academy of Sciences. He recently received an Alcon Research Institute recognition award for outstanding research in ophthalmology.



RUSSELL L. McCALLY was born in Marion, Ohio. He received a B.Sc. degree in physics from Ohio State University in 1964 and shortly thereafter joined APL's Aeronautics Division, where he was involved in research on explosives initiation. In 1969, he joined the Theoretical Problems Group in APL's Milton S. Eisenhower Research Center. He received M.S. (1973) and M.A. (1983) degrees in physics from The Johns Hopkins University, and in 1979-80 was the William S. Parsons Fellow in the Physics Department. Mr. McCally's research interests include the application of light scattering meth-

ods to the study of corneal structure, the physics of laser-tissue interactions, and magnetism in amorphous alloys. He is co-principal investigator on a grant from the National Eye Institute that supports corneal light scattering research. His professional memberships include the American Physical Society and the Association for Research in Vision and Ophthalmology.



DAVID E. FREUND is a physicist in the Theoretical Problems Group. He joined APL's Milton S. Eisenhower Research Center in 1983. Born in Hamilton, Ohio, he received a B.A. degree from Lycoming College in 1972, an M.S. degree from Purdue University in 1974, and a Ph.D. degree from the University of Delaware in 1982. Dr. Freund's research interests include developing theoretical methods for calculating acoustic and electromagnetic wave scattering in random media and the use of light scattering for probing the ultrastructure of the cornea.